Soft Matter

COMMUNICATION

View Article Online
View Journal | View Issue

Cite this: *Soft Matter*, 2016, 12, 7259

Received 19th May 2016,
Accepted 6th August 2016

DOI: 10.1039/c6sm01162d

www.rsc.org/softmatter

Pattern formation in chemically interacting active rotors with self-propulsion†

Benno Liebchen,*[a] Michael E. Cates[b] and Davide Marenduzzo[a]

We demonstrate that active rotations in chemically signalling particles, such as autochemotactic *E. coli* close to walls, create a route for pattern formation based on a nonlinear yet deterministic instability mechanism. For slow rotations, we find a transient persistence of the uniform state, followed by a sudden formation of clusters contingent on locking of the average propulsion direction by chemotaxis. These clusters coarsen, which results in phase separation into a dense and a dilute region. Faster rotations arrest phase separation leading to a global travelling wave of rotors with synchronized roto-translational motion. Our results elucidate the physics resulting from the competition of two generic paradigms in active matter, chemotaxis and active rotations, and show that the latter provides a tool to design programmable self-assembly of active matter, for example to control coarsening.

Various self-propelled microorganisms, like the bacterium *E. coli*[1–3] or the slime mold *Dictyostelium disoideum* (Dicty)[4] can adapt their motion in response to gradients of chemicals which they produce themselves (Fig. 1a). Such a chemical 'signalling' can induce spontaneous aggregation through a positive feedback (Fig. 1b): an initial positive chemical density fluctuation attracts microorganisms, which produce further chemicals; this amplifies the initial fluctuation supporting the recruitment of further microorganisms, which eventually condense into a macroscopic cluster coexisting with a dilute microbial bath (Fig. 1b). Quantified by the Keller–Segel (KS) model in the 1970s,[5,6] this signalling-route to phase separation now serves as a prototypical example for self-organization in nonequilibrium.[7] It is crucial for the life cycle of Dicty;[4] it is also one possible mechanism to explain pattern formation in bacterial colonies within agar,[1,2] alongside an alternative explanation based on arrested motility induced phase separation.[8]

Currently, the KS instability is attracting renewed attention in active synthetic Janus colloids. These particles catalyse reactions within a chemical bath, yielding gradients which drive self-propulsion *via* diffusiophoresis or a similar mechanism. Importantly, other colloids may feel rotational torques caused by the same long-ranged gradients and respond to them by adapting their swimming direction, thereby providing a synthetic analog of chemotactic signalling.[9–11] The same KS equations can therefore be transferred from the microbiological world to phoretic colloids.[10,12–14] Here, either the KS instability, or instabilities based on chemorepulsion[15] may help explain the still elusive dynamic clustering observed in experiments.[10,16,17]

In all these cases chemotactic instability relies on the ability of weak chemical fluctuations around the uniform density to align microswimmers up (or down) chemical gradients. However, under many circumstances microswimmers vary their swimming direction autonomously of chemical cues: this occurs, *e.g.*, for bacteria swimming clockwise close to a glass wall,[18] or anti-clockwise near an oil–water interface[19] (see ESI† for a discussion on parameters). Synthetic examples of active signalling rotors with self-propulsion (sometimes called 'circle swimmers') may be realised with L-shaped phoretic swimmers,[20,21] or with active particles with dipole moments[16,22,23] which will track the rotation of applied external fields[16,24] and can interact *via* self-produced phoretic fields.[16]

We should expect that, close to uniform states, finite active torques as caused by intrinsic rotations will generally outcompete chemotactic torques which are proportional to the chemical gradient, when it comes to determining swimming direction: hence, they might generically lead to a breakdown of the linear KS instability. Does this rule out the possibility of phase separation and patterning in signalling rotors? This could have profound consequences for systems like thin (bio)films of chemotactic bacteria[25] or actuated phoretic particles.

Here, we propose a generic model to study active signalling rotors. As a key result we find that even weak active rotations suppress the linear KS instability. However, we identify an instability mechanism which is distinct from the KS mechanism

[a] *SUPA, School of Physics and Astronomy, University of Edinburgh, Edinburgh EH9 3FD, UK. E-mail: Benno.Liebchen@staffmail.ed.ac.uk*
[b] *DAMTP, Centre for Mathematical Sciences, University of Cambridge, Cambridge CB3 0WA, UK*

† Electronic supplementary information (ESI) available. See DOI: 10.1039/c6sm01162d

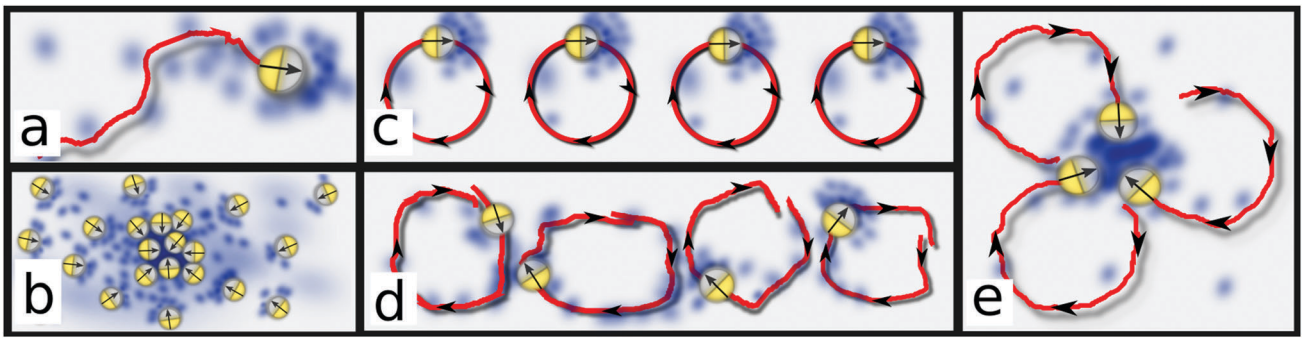

Fig. 1 Cartoons showing the basic setup and the locking instability (see text). (a) Chemotactic colloid/bacterium swimming up a self-produced chemical gradient. (b) Keller–Segel instability. (c) Uniform phase of coherent rotors. (d) Rotors leave chemical trail dephasing coherent rotations. (e) Possible seed configuration for the locking instability.

and creates a nonlinear, but deterministic, route to pattern formation.

For small rotation frequency, this route generates macroscopic phase separation: a fraction of the rotors condenses into a dense phase, separated from a dilute gas by a quasi-stationary interface where chemotaxis suppresses rotations and 'locks' the average swimming direction onto the upward density gradient. Away from the interfaces, rotations persist in both phases and lead to dynamic patterns, such as spots or moving stripes and spirals (Fig. 2h and i) This combination of phase separation with pattern formation within both phases represents a novel type of hierarchical structure formation. When increasing the rotation frequency above a certain threshold, strikingly, the growing clusters do not coarsen any more but form a global pattern of travelling stripes with self-limiting size, suggesting that active rotations can be used to control coarsening in suspensions of self-propelled particles (Fig. 2l).

We describe active particles which self-propel with velocity v_0 and rotate with frequencies $\omega_i > 0$ at a coarse grained level in two-dimensions. A smooth $\rho(\mathbf{x},t)$ represents the active particle density and $\mathbf{p}(\mathbf{x},t)$ is the local average of the unit vector describing the direction of self-propulsion. We focus on polarized rotors with identical frequencies, which applies to synthetic colloidal rotors locked to a rotating field, but also to bacterial rotors where short-ranged alignment interactions can synchronize the individual rotations locally (see ESI† and final paragraph). Thus, in absence of signalling, $\mathbf{p}$ rotates with a collective frequency ω. Generally however, our rotors produce signalling

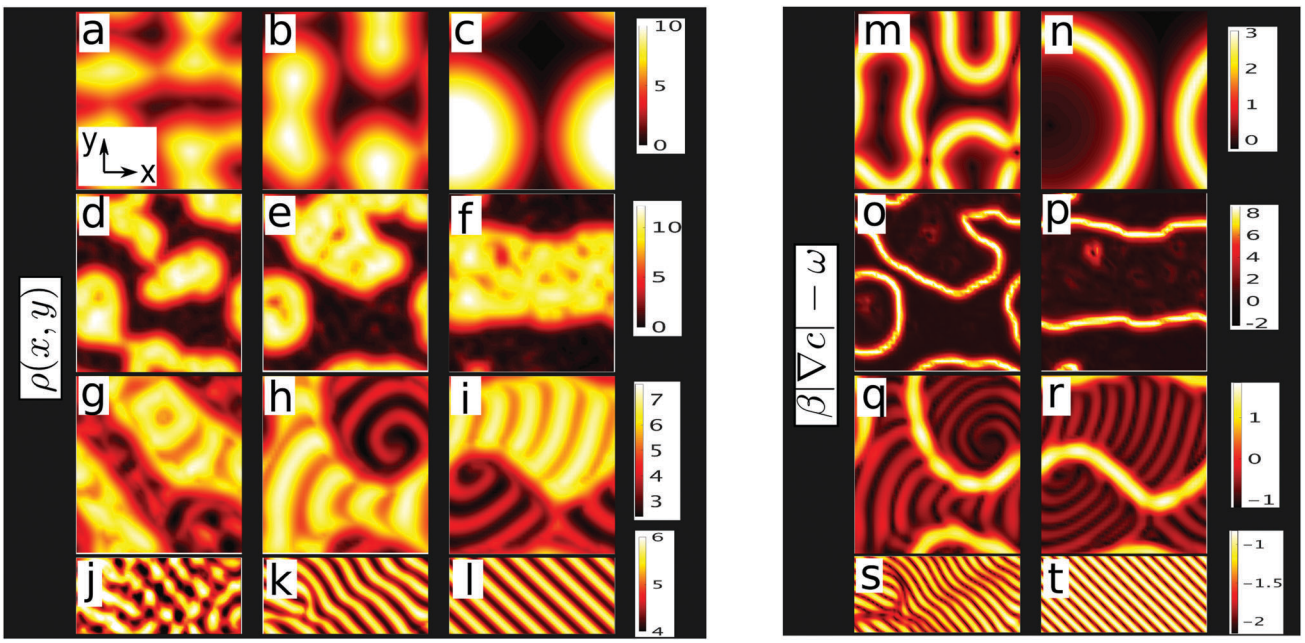

Fig. 2 (a–l) Snapshots of density field ρ for different free rotation frequencies ω as a function of x, y at different times (increasing from left to right). Values for ω and Δ are: $\omega = 0$; $\Delta = 0$ (a–c); 0.25; 5×10^{-3} (d–f); 1.2; 0.024 (g–i) and 2.2; 0.044 (j–l). (m–t) Snapshots of $\beta|\nabla c| - \omega$ corresponding to the density fields of columns 2 and 3 (m belongs to b; n to c *etc.*). Positive values represent locking, negative values rotations. Parameters: $\beta = 5.0$, $\rho_0 = 5.0$, $v_0 = 0.5$, $k_d = k_0 = 1$, $\varepsilon = 10$, $D_\rho = 0.417$; $K = 0.025$; $D_c = 1$; $c_0 = (k_0/k_d)\rho_0$; $L_x \times L_y = 50 \times 50$ in the first and third row, 40×40 in the second row and 80×32 in the fourth row; $0.32\sqrt{D_\rho/k_d}$ is the distance between adjacent gridpoints.

molecules with a local rate $k_0\rho$; hence $\mathbf{p}$ also responds, *via* chemotaxis, to gradients of the resulting chemical field $c(\mathbf{x},t)$, which is degraded with a rate k_d (compare ref. 5 and 26). This yields a competition of intrinsic active rotations and chemotactic alignment which determines the behaviour of the signalling rotors at large scales. Allowing for finite diffusion of the chemical and colloidal density fields with coefficients D_c and D_ρ, we describe signalling rotors phenomenologically by:

$$\dot{\rho} = -v_0\nabla\cdot(\rho\mathbf{p}) + D_\rho\nabla^2\rho + K\nabla^2\rho^3 \quad (1)$$

$$\dot{\phi} = \omega + \beta\hat{\mathbf{p}}\times\nabla c; \quad \mathbf{p} = (\cos\phi, \sin\phi)^T \quad (2)$$

$$\dot{c} = k_0\rho - k_d c + D_c\nabla^2 c + \varepsilon(c_0 - c)^3. \quad (3)$$

Here, we used the notation $\mathbf{a}\times\mathbf{b} = a_1b_2 - a_2b_1$ and introduced a chemotactic coupling strength β, as well as an isotropic short range repulsion among colloids of strength $K > 0$ and a cubic reaction term with rate coefficient ε leading to the saturation of any unstable mode.[27] This phenomenological model can be justified microscopically using the closure scheme of ref. 28 and some further approximations discussed in the ESI.† Our model is studied here as a minimal description of chemotactic rotors, which focuses on the competition between chemotaxis and active rotations. Its parameter space can be reduced to five dimensions (ESI†) including the effective density $\rho_0k_0\beta/(k_dv_0)$ which is conserved in the course of the dynamics and $\Omega = \omega/k_d$ measuring the number of rotational cycles in absence of chemotaxis during the characteristic degradation time of c. Together with $\mathscr{D}_c = D_c/D_\rho$ which measures the ratio of chemical and colloidal/bacterial diffusion, both mainly affecting length scales here, these parameters determine the linear behaviour of the present model. The two remaining parameters $\kappa = Kk_d^2v_0^2/(D_\rho k_0^2\beta^2)$ and $\varepsilon = \varepsilon v_0^2/(k_d\beta^2)$ control non-linear effects. We choose experimentally sensible values for these parameters (ESI†) and introduce the dimensionless number $\Delta = \omega v_0/(\rho_0k_0\beta)$ as a measure of the relative importance of active rotations (circular swimming) and chemotaxis (biased swimming up chemical gradients) as our key control parameter.

We now explore the competition of active rotations and chemotaxis by solving eqn (1)–(3) for different Δ on a square lattice with $L_x \times L_y$ grid points and periodic boundary conditions using finite difference methods. As an initial state, we choose a small and random perturbation of the spatially uniform and coherently rotating state $(\rho,\phi,c) = (\rho_0,\omega t,(k_0/k_d)\rho_0)$ which solves eqn (1)–(3). In absence of rotations ($\Delta = 0$) we observe clusters growing out of the uniform state (Fig. 2a), which colocalise with chemical density maxima and coarsen at long times (Fig. 2b), yielding one dense macroscopic cluster coexisting with a dilute gas (Fig. 2c). Here, instability of the uniform state is expected due to the positive feedback loop of particle aggregation and chemical production we discussed in the introduction and in ref. 15.

For $\Delta = 5\times10^{-3}$ this picture changes dramatically. Now the uniform state persists for a certain duration (see Videos 1 and 2 in ESI†): we call this the initial lag regime. Then, almost suddenly, fluctuations 'awake' and grow to create clusters (Fig. 2d). These clusters coarsen into a relatively dense phase separated from a dilute rotor gas (Fig. 2f) by a slowly-moving interface where rotations are suppressed and particles swim, on average, up the chemical gradient (Video 2, ESI†). Away from the interface, all colloids perform a 'stop-and-go' rotation, which is associated with dynamic short-lived density dips and peaks (white spots and red dips in yellow region in Fig. 2e and f). Choosing stronger rotations ($\Delta = 0.024$) we observe a similar suppression of rotations at the interfaces, but within both phases stripe and spiral patterns form (Fig. 2g–i and Video 2, ESI†).

For $\Delta = 0.044$ complexity suddenly breaks down: after a long initial lag regime and an intermediate regime where short-lived dynamic clusters continuously emerge and decay, we find a travelling wave made of straight parallel stripes (Fig. 2k and l, Video 4, ESI†) with self-limiting wavelength. This sudden emergence of a length scale upon increasing Δ allows control of coarsening *via* active rotations. The length scale of the stripe pattern which decreases as ω increases and thus can be also controlled.

Rotation-locking transition

To understand the origin of cluster growth for $\Delta > 0$ and the related suppression of rotations at the cluster interfaces, we recast eqn (2) as

$$\dot{\phi} = \omega + \beta|\nabla c|\sin(\phi + \delta); \quad \delta = \arg(-\partial_x c + \mathrm{i}\partial_y c) \quad (4)$$

Assuming a time-independent chemical field this can be read, locally, as the Adler equation of synchronization theory which features a transition from (quasi-)periodic rotations ($\beta|\nabla c| < \omega$) to phase locking ($\beta|\nabla c| > \omega$), see ESI† and ref. 29–31. Although, for our signalling rotors ∇c, hence also δ, evolve in time, in the parameter regime relevant to our numerical simulations, $\mathbf{p}$ responds fast to changes in c, hence we expect that the locking transition should still apply (ESI†). Our simulations confirm this expectation and clearly show a transition from 'active' rotations to locking at $\beta|\nabla c| \approx \omega$ (Fig. 2o and r), which explains the suppression of rotations at, and only at, the interface in Fig. 2e–i, where chemical gradients are strong enough to generate locking. This locking induces a permanent self-advective flux of particles from the dilute phase to the dense phase balancing diffusion in the opposite direction and thus stabilizes dense rotor clusters. Hence, steep enough interfaces maintain themselves and allow only for small fluctuations of $\beta|\nabla c| - \omega$ in the course of the further dynamics.

Locking instability

Since the locking mechanism stabilizes clusters, we expect an instability mechanism allowing for the growth of these clusters out of the uniform state. We now resolve this in detail. Working in the adiabatic limit where $\mathbf{p}$ responds fast to changes of c, eqn (1)–(3) simplify significantly. If $\omega = 0$, they resemble the Keller–Segel model (ESI†), which leads to phase separation through a long wavelength linear instability – essentially this is the positive feedback described in the Introduction. In sharp

contrast, we show in the ESI† that active rotations generically suppress linear instability of the uniform phase in eqn (1)–(3). Physically, this is in line with the intuitive expectation that small chemical gradients caused by fluctuations around the uniform state are too weak to fix the orientations of active rotors and cannot promote a linear instability. As a result, the KS instability is ineffective for active signalling rotors.

This raises the question why we could still observe cluster growth in our simulations. The answer is that chemotaxis can abduct the rotors into the nonlinear regime before they complete a full rotation, and this in turn can lead to a nonlinear instability. To understand the underlying physical mechanism, let us reconsider our coherently rotating uniform initial state, where all rotors are in phase (Fig. 1c). While ρ, c remain approximately uniform in the course of the early-stage dynamics, weak fluctuations of c continuously dephase the orientation field $\mathbf{p}$ due to chemotaxis (Fig. 1d). Once the rotors are sufficiently out of phase, they can form, temporarily, aster-like 'seed' configurations (Fig. 1e), where all particles in the vicinity of a positive fluctuation of c swim up the chemical gradient. This configuration promotes, temporarily, a growth of the fluctuation *via* the standard KS feedback loop. If this growth generates a chemical gradient surpassing the locking-threshold ($\beta|\nabla c| > \omega$) before the seed decays, then $\mathbf{p}$ remains locked in its vicinity – leading to a stable cluster as just discussed.[35] Hence, we call our nonlinear instability the 'locking instability'. Whether the locking instability is effective or not in practice is a matter of competing timescales, between the instantaneous growth rate of chemical gradients and ω – the former needs to dominate to create locking. Video 5 in the ESI† shows the early stage dynamics of c and $\mathbf{p}$, reflecting that c and its gradients can indeed grow beyond the locking threshold on timescales where $\mathbf{p}$ rotates only slightly.

Breakdown of locking

Locking gets increasingly difficult as Δ increases and eventually breaks down, quite suddenly, at $\Delta \approx 0.027$ (for parameters as in Fig. 2); beyond this, stable clusters are no longer possible. Specifically, as Δ increases (i) steeper interfaces are needed to satisfy the locking criterion and (ii) active rotations increasingly dominate the equilibrium between chemotaxis and rotations which leads to a steering of the locked $\mathbf{p}$ away from its 'ideal' orientation up the gradient. This in turn reduces the advective flux up the density gradient leading to shallower interfaces (see ESI† and Videos 2 and 3). Unlike for linear (supercritical) instabilities an instability criterion is ill-defined here, and the breakdown of locking depends on an implicit balance between steepness of interfaces and locking orientation of $\mathbf{p}$ far away from the uniform state. Likewise, when comparing the locking instability to nucleation in systems approaching thermal equilibrium, which is also nonlinear and requires a seed configuration, we find again important differences. Crucially, for example, our clusters require steep interfaces to survive, and a dense cluster with shallow interfaces would quickly decay; in contrast, for near-equilibrium systems, once a dense seed has nucleated it will grow, however shallow its interfaces may be.

Active rotations arrest coarsening

For large Δ, where rotations are too strong to allow locking, we observed a long period where small and short lived clusters dynamically emerge and decay on timescales $\sim 2\pi/\omega$. These clusters emerge from seeds which promote a growth of ρ and c which is too slow to surpass the locking threshold and hence slows down the rotation of $\mathbf{p}$ only temporarily. Strikingly, however, this dynamic clustering does not proceed forever, and eventually some clusters merge (due to diffusion and short ranged repulsions which penalize large interfaces) and synchronise their rotations and translations to form coherent waves (see Video 4 in ESI†). Specifically, within clusters, the relative phases (frequencies) of adjacent rotors change continuously until the system eventually reaches a steady state. Here such a steady state is possible in the form of a stripy pattern (Fig. 2l), which moves precisely by one spatial period during one rotational cycle of $\mathbf{p}$. In a frame comoving with the pattern, $\mathbf{p}$ is then fixed (Fig. 3b) and the pattern, a periodic non-uniform state, is an attractor for the dynamics of the system. Hence, merging and approaching this steady state represents a second route allowing short lived clusters to avoid decay.

This process of forming short lived clusters which prevent their decay by merging and moving into a collective direction (spontaneous symmetry breaking) constitutes a second nonlinear instability mechanism of the uniform state that is independent of the locking mechanism. In contrast with the latter, this mechanism works at all frequencies, but is comparatively slow since it involves the coordination of several clusters. Hence this second route to structure formation in signalling rotors is particularly relevant in parameter regimes where the locking mechanism is ineffective, *i.e.*, for large ω, but applies similarly to the moving stripes formed within the dense and the dilute phase in Fig. 2g–i.

As its most remarkable feature and contrasting the locking instability, this route to pattern formation introduces a length scale in steady state. Within a large region of parameter space, this length scale increases approximately as v_0/ω. Hence, for

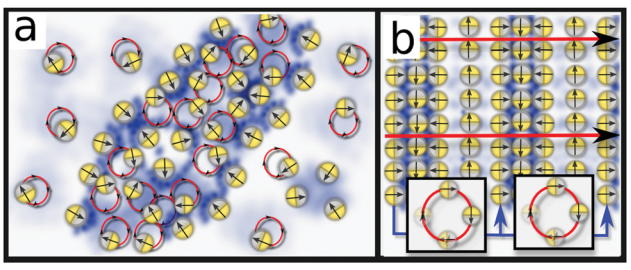

Fig. 3 Schematics of possible asymptotic states (see text) (a) slow rotations: macrophase separation with coexisting dilute and dense phase of rotors separated by an interface of chemically locked rotors. (b) Moderate rotations: travelling wave pattern of signalling rotors with synchronized rotational and translational motion of $\mathbf{p}$.

synthetic rotors this length scale can be tuned *via* the frequency of an applied rotating field. We emphasize that this length scale is determined purely dynamically and cannot be calculated *via* the standard tools for linear (supercritical) instabilities like amplitude equations.[32]

Non-identical frequencies

We finally discuss signalling rotors with non-identical frequencies (*e.g.*, a population of bacteria close to a wall). In absence of alignment effects these rotors quickly dephase and destroy the local polar order. However, hydrodynamic[33] or steric alignment interactions can 'synchronize' individual rotations. Assuming, *e.g.*, short ranged polar alignment interactions with alignment rate $(g/r_c^2)\sin(\theta_j - \theta_i)$ between particles i,j (polar coordinates) if their distance $|\mathbf{r}_i - \mathbf{r}_j|$ is smaller than a cutoff radius r_c and ignoring chemotaxis (which supports alignment), the local orientation of a rotor follows

$$\dot{\theta}_i = \omega_i + \sqrt{2D_r}\xi_i(t) + \left(g/r_c^2\right)\sum \sin\left(\theta_j - \theta_i\right) \qquad (5)$$

Here we sum over all $N_c \approx r_c^2\rho(\mathbf{r}_i)$ particles with distance less than r_c to the ith particle and $\xi_i(t)$ represents unit-variance Gaussian white noise. Remarkably, for dense systems, eqn (5) can be identified (locally) as the Kuramoto model with noise[34] which shows a phase transition from the incoherent uniform phase to frequency locking if $g\rho_0$ is a few times larger than D_r and the standard deviation Δ_ω of the distribution function of the individual frequencies.[34] Thus, within an ensemble of non-identical rotors, a strong enough alignment interaction causes a macroscopic fraction of them to rotate in phase with an average frequency, so that our analysis for identical rotors still largely applies. The main caveat is that synchronization of the individual rotations takes place locally, so the average rotation may vary in space and time. We thus performed simulations of eqn (1)–(3) with additional frequency noise $\omega_\xi(\mathbf{x}, t)$ in eqn (2): the results resemble those in Fig. 2 as long as $\Delta_\omega < \omega$ and the correlation time of ω_ξ is short compared to $1/\omega$. Note, that the ESI† material provides an alternative and direct microscopic justification of eqn (1)–(3) for rotors with non-identical frequencies. We finally remark that our model (eqn (1)–(3)) can be viewed as an extension of motile oscillators,[36,39] which are known to feature travelling waves,[37,38] to cases where the phase dynamics influences the spatial dynamics of individual oscillators.

In conclusion, although even weak active rotations linearly stabilise the uniform phase in ensembles of auto-chemotactic particles, they generate a nonlinear route to structure formation. This route creates novel patterns including hierarchically organized states combining phase separation and pattern formation. It also allows for features which would be impossible to achieve in linear instability scenarios, such as a delayed onset of patterning whose lag time can be programmed *via* the initial conditions. More generally, we showed that rotations provide a versatile new tool to design self-assembly and collective behaviour of active matter, for example to control coarsening.

Acknowledgements

BL gratefully acknowledges funding by a Marie Skłodowska Curie Intra European Fellowship (G.A. no. 654908) within Horizon 2020. MEC holds a Royal Society Research Professorship. Work funded in part by EPSRC EP/J007404/1.

References

1 E. O. Budrene and H. C. Berg, *Nature*, 1991, **349**, 630.
2 E. O. Budrene and H. C. Berg, *Nature*, 1995, **376**, 49.
3 N. Mittal, E. O. Budrene, M. P. Brenner and A. Van Oudenaarden, *Proc. Natl. Acad. Sci. U. S. A.*, 2003, **100**, 13259.
4 G. Gerisch, *Annu. Rev. Physiol.*, 1982, **44**, 535.
5 E. F. Keller and L. A. Segel, *J. Theor. Biol.*, 1970, **26**, 399.
6 E. F. Keller and L. A. Segel, *J. Theor. Biol.*, 1971, **30**, 225.
7 H. Haken, *The Science of Structure: Synergetics*, Van Nostrand Reinhold Company, 1984.
8 M. E. Cates, D. Marenduzzo, I. Pagonabarraga and J. Tailleur, *Proc. Natl. Acad. Sci. U. S. A.*, 2010, **107**, 11715.
9 Y. Hong, N. M. K. Blackman, N. D. Kopp, A. Sen and D. Velegol, *Phys. Rev. Lett.*, 2007, **99**, 178103.
10 I. Theurkauff, C. Cottin-Bizonne, J. Palacci, C. Ybert and L. Bocquet, *Phys. Rev. Lett.*, 2012, **108**, 268303.
11 S. Saha, R. Golestanian and S. Ramaswamy, *Phys. Rev. E: Stat., Nonlinear, Soft Matter Phys.*, 2014, **89**, 062316.
12 J. Taktikos, V. Zaburdaev and H. Stark, *Phys. Rev. E: Stat., Nonlinear, Soft Matter Phys.*, 2012, **85**, 051901.
13 M. Meyer, L. Schimansky-Geier and P. Romanczuk, *Phys. Rev. E: Stat., Nonlinear, Soft Matter Phys.*, 2014, **89**, 022711.
14 O. Pohl and H. Stark, *Phys. Rev. Lett.*, 2014, **112**, 238303.
15 B. Liebchen, D. Marenduzzo, I. Pagonabarraga and M. E. Cates, *Phys. Rev. Lett.*, 2015, **115**, 258301.
16 J. Palacci, S. Sacanna, A. P. Steinberg, D. J. Pine and P. M. Chaikin, *Science*, 2013, **339**, 936.
17 I. Buttinoni, J. Bialké, F. Kümmel, H. Löwen, C. Bechinger and T. Speck, *Phys. Rev. Lett.*, 2013, **110**, 238301.
18 E. Lauga, W. R. DiLuzio, G. M. Whitesides and H. a. Stone, *Biophys. J.*, 2006, **90**, 400.
19 R. Di Leonardo, D. Dell'Arciprete, L. Angelani and V. Iebba, *Phys. Rev. Lett.*, 2011, **106**, 038101.
20 F. Kümmel, B. ten Hagen, R. Wittkowski, I. Buttinoni, R. Eichhorn, G. Volpe, H. Löwen and C. Bechinger, *Phys. Rev. Lett.*, 2013, **110**, 198302.
21 M. Wykes, J. Palacci, T. Adachi, L. Ristroph, X. Yhong, M. Ward, J. Zhang and M. Shelley, 2015, arXiv:1509.06330v1 [cond-mat.soft].
22 L. Baraban, D. Makarov, O. G. Schmidt, G. Cuniberti, P. Leiderer and A. Erbe, *Nanoscale*, 2013, **5**, 1332.
23 L. Baraban, R. Streubel, D. Makarov, L. Han, D. Karnaushenko, O. G. Schmidt and G. Cuniberti, *ACS Nano*, 2013, **7**, 1360.
24 N. H. P. Nguyen, D. Klotsa, M. Engel and S. C. Glotzer, *Phys. Rev. Lett.*, 2014, **112**, 075701.
25 H. C. Berg and L. Turner, *Biophys. J.*, 1990, **58**, 919.
26 J. Murray, *Mathematical Biology. II: Spatial Models and Biomedical Applications, Springer-Verlag Berlin*, 2003.

27 While we chose a cubic interaction term in analogy with the ϕ^4 theory, a quadratic interaction term $\propto \nabla^2\rho^2$ with appropriately increased coefficient does not change our results. Similarly, replacing the cubic reaction term by *e.g.* a quadratic, sign-changing term $\propto (c_0 - c)|c_0 - c|$ has very little bearing on our results. (A quadratic, non sign-changing term $\propto (c_0 - c)^2$ would lead to a blowup of fluctuations rather than to their saturation).
28 E. Bertin, M. Droz and G. Grégoire, *J. Phys. A: Math. Theor.*, 2009, **42**, 445001.
29 R. Adler, *Proc. IRE*, 1946, **34**, 351.
30 A. Pikovsky, M. Rosenblum and J. Kurths, *Synchronization: A Universal Concept in Nonlinear Sciences*, Cambridge University Press, 2003.
31 T. Erneux and P. Glorieux, *Laser Dynamics*, Cambridge University Press, 2010.
32 P. C. Hohenberg and M. C. Cross, *Rev. Mod. Phys.*, 1993, **65**, 851.
33 R. Golestanian, J. M. Yeomans and N. Uchida, *Soft Matter*, 2011, **7**, 3074.
34 J. A. Acebrón, L. L. Bonilla, C. J. P. Vicente, F. Ritort and R. Spigler, *Rev. Mod. Phys.*, 2005, **77**, 137.
35 Note that in contrast to asters, 'anti-asters' with p pointing outwards from a center where ρ, c show minima, suffer from the fact that both ρ, c cannot decay below zero. This limits the maximal possible steepness of chemical gradients to values which are typically insufficient to generate locking.
36 J. Ito and K. Kaneko, *Phys. Rev. Lett.*, 2001, **88**, 028701.
37 F. Peruani, E. M. Nicola and L. G. Morelli, *New J. Phys.*, 2010, **12**, 093029.
38 K. Uriu, S. Ares, A. C. Oates and L. G. Morelli, *Phys. Rev. E: Stat., Nonlinear, Soft Matter Phys.*, 2013, **87**, 032911.
39 R. Grossmann, F. Peruani and M. Bär, *Phys. Rev. E*, 2016, **93**, 040102.

